Eur. Phys. J. Appl. Phys. **42**, 311–319 (2008)
DOI: 10.1051/epjap:2008062

THE EUROPEAN PHYSICAL JOURNAL
APPLIED PHYSICS

# Focussing of a transient low energy $Cs^+$ probe for improved NanoSIMS characterizations

## Study of charged particle optics*

M. Bernheim[1,a], T.D. Wu[2,3], J.L. Guerquin-Kern[2,3], and A. Croisy[2,3]

[1] Laboratoire de Physique des Solides, Univ. Paris-Sud, UMR CNRS 8502, 91405 Orsay, France
[2] Institut Curie, Laboratoire de Microscopie Ionique, 91405 Orsay, France
[3] INSERM, U759, 91405 Orsay, France

Received: 10 January 2008 / Received in final form: 13 February 2008 / Accepted: 4 March 2008
Published online: 30 April 2008 – © EDP Sciences

**Abstract.** Surface caesium content is known to greatly influence the negative ion yield during SIMS analyses. In NanoSIMS, a 16 keV ion probe of $Cs^+$simultaneously performs the surface enrichment and the sample sputtering. To increase the surface caesium content and thus generate higher ion yields, it is suggested herein to significantly reduce the energy of the primary ions by biasing the sample with a positive voltage slightly smaller than the voltage of 8000 V that is used for primary ion acceleration. Then, once the typical bias voltages are restored, SIMS analysis may carried out with increased sensitivity right from the beginning of the sample erosion. The use of such a procedure may improve many types of SIMS investigations such as thin sections of biological samples, semiconductor wafers shallowly doped over very small areas and small meteorite samples. However, during deceleration close to the sample surface, the beam size is markedly enlarged unless the excitation of the objective lens is corrected. In this study, optics simulations are performed using Simion 8 in order to facilitate adjustment of the experimental setups. An objective lens excitation set at $E0P = 0$ V and $E0S = +5930$ V focuses a 100 eV caesium beam into an area 9.2 $\mu$m in diameter. Even for a final energy as low as 25 eV, 90% and 50% of the beam is confined to areas of 30 $\mu$m and 4 $\mu$m in diameter respectively (with electrodes $E0P$ and $E0S$ set at 3150 and 5450 V and using a beam slightly limited in angle). The procedures being suggested will be confirmed by experimental studies soon to be submitted as complementary contribution. As predicted, caesium rich surfaces greatly improve ion yield and consequently localised SIMS analysis as well.

**PACS.** 68.37.-d Microscopy of surfaces, interfaces, and thin films – 79.20.Rf Atomic, molecular, and ion beam impact and interactions with surfaces Electron and ion channeling – 87.64.-t Spectroscopic and microscopic techniques in biophysics and medical physics

## 1 Introduction

### 1.1 Optical configurations

Several different experimental setups employ immersion objective lenses working in a coaxial mode with various beams of charged particles directed along the same optical axis but in opposite directions:

– In IMS (n)F[1] setups, measurements based on emissions of negative secondary ions have been extended to insulating samples by including an auto-regulating surface potential control performed by an auxiliary electron beam applied to the objective lens in mirror-like conditions [1].
– A similar configuration has been used to apply an electron beam of constant density and of adjustable energy to trigger desorption of negative ions that are collected with high efficiency through the objective lens. Such conditions are well suited for ESD studies and especially for the investigation of the resonant desorption of negative ions stimulated by electron impact at energies below 10 eV [2].
– Finally in NanoSIMS setup as well, a coaxial lens system is used both to focus a narrow probe of primary ions over the studied surface and to efficiently collect the secondary ions. Unlike the direct acquisitions of ion images used in other SIMS setups, the surface

* The correlated experiments will be reported soon in part B.

[a] e-mail: bernheim@lps.u-psud.fr

[1] IMS(n)F and NanoSims are mass spectrometers which are dedicated to localised SIMS analysis and are built by the CAMECA company. G. Slodzian played a crucial role in the definition, in the development and in the application of the successive apparatuses.

images are reconstructed sequentially from the output of the mass-spectrometer working in multi-detection mode and with high mass resolution. Here the objective lens conveys two beams of opposite electric charges: an ion probe made up of positive caesium ions post-accelerated from 8 keV to 16 keV, and negative secondary ions accelerated to 8 keV before their admission into the mass-spectrometer [3].

### 1.2 Caesium influence on negative ion yield

It is well-known that just as with any other alkaline element, caesium greatly increases the amount of negative ions among the particles ejected during sputtering. Therefore, caesium-rich surfaces improve localised SIMS analyses for elements of very low concentration ejected as negative ions[2] from heterogeneous samples. This increased sensitivity is crucial as SIMS analysis is a destructive process and therefore cannot be repeated in the same place and for the very same atoms.

Since the negative ion yield varies sharply with the surface concentration of caesium, the most precise measurements are performed under experimental conditions which consist of a specific dynamical equilibrium: a beam of noble gas ions performs a continuous surface sputtering, while a neutral caesium beam forms chemisorbed overlayers of adjustable surface concentration [4,5].

Indeed it has been shown that an increase in caesium surface concentration causes a quasi exponential growth in both ion yield and in negative ion occurrence probability up to a maximum effectiveness corresponding to the highest possible reduction in surface work function. For negative ions, the offset of the energy distribution provides an in situ access to the surface work function for various coverages of caesium [6].

Under the previous sputtering equilibrium conditions, ion scattering spectrometry (ISS) may also give complementary information about the surface compositions as this can be deduced from the height of the binary collisions peaks. This procedure exploits the fact that neon ions scattered with high enough energy escape most surface neutralisations. The use of such ion species is convenient – especially for ISS – provided that a mass filter isolates a single isotope as incident ions. For a scattering angle of 135° and for $^{20}Ne^{+}$ ions directed with 10 keV onto a copper crystal, the intensity of the two $^{20}Ne^{+}$peaks at 3125 eV and 5880 eV vary with the atomic concentrations of [Cu] and [Cs] during the previous described dynamical equilibrium conditions. The highest ion yield of $Cu^{-}$ ions and the lowest work function were shown to correspond to a surface atomic concentration of 0.25 Cs at., which is in fair agreement with measurements deduced from photoemission studies performed under static conditions on the same surfaces [6–9].

Once the caesium coverage is adjusted to achieve the work function minimum, the measured ion yield varies vary proportionally with the atomic concentrations including an exponential dependence on the element electron affinity. Such conditions provide easy quantitative analyses that are truly free of "matrix effects"[3].

In practice, the beam of neutral caesium should be collimated in order to avoid any deposition outside of the eroded surface [4,5]. Such a constraint may not be compatible with the NanoSIMS configuration.

In addition, $Cs^{+}$ primary ion probes with energies as high as 16 keV are inconvenient for the characterization of the very surface compositions initially free of alkaline elements.

Indeed, a significant initial ion dose is needed to sufficiently enrich the surface with caesium and thus to access high negative ion yields. In practice, after a transitory regime, a dynamical equilibrium is reached where the caesium concentration is about $1/(S+1)$, $S$ being the sputtering yield, defined as the average number of target atoms and molecules ejected per primary ions. Due to the high sputtering yield of caesium at 16 keV, the equilibrium concentration remains far too low to contribute a high secondary ion yield.

For example during the azimuth rotation, the lattice transparency contrast determines the sputtering yield for the (100) face of a single crystal copper sample when a caesium ion beam of 10 keV is applied at incidence angle of 45°.

At equilibrium, variations in sputtering yields and in caesium surface content cause significant differences in the work functions as observed for both opaque and transparent azimuths. Large variations in the ion yields of $Cu^{-}$ are detected consequently. However, a complementary surface Cs supply (as provided with a neutral caesium beam) causes additional reductions of 1.4 eV and 2.7 eV in work function so that an identical saturation state now provides identical concentrations and work functions. This complementary caesium supply markedly increases the $Cu^{-}$ yield by factors up to 100 in the opaque position [10].

### 1.3 Practical constraints for biological-samples

The NanoSIMS setup was mainly developed for the localised analysis of biological tissues while providing high spatial resolution and sensitivity. Due to their high energy, primary caesium ions have very long ranges in biomaterials which are composed of light elements. Therefore, the creation of a caesium rich surface implies a significant

[2] When sputtered elements or polyatomic species have electron affinities they may leave the sample as negative ions.

[3] Once this dynamical equilibrium is reached, the primary particle content depends primarily on the sputtering yield. When reactive species (Cs, O, ...) are used as reactive primary ions directly, consecutive variations in secondary ion yields are called "matrix effects". A distinct matrix effect is observed on metal alloys excluding chemical environment (the yields of positive ions being influenced by atomic concentration of other element). Also geological samples like silicate compounds exhibit similar matrix effects, each species having a yield influenced by the atomic composition of the other species.

ion dose. Such conditions may trigger element redistributions in the uppermost layers of the sample. During the ion collision cascades secondary electrons may also contribute to atom redistributions close to the sample surface.

This study aims to evaluate how a caesium beam with a very low final energy could be applied transitorily to build a caesium rich surface under "soft landing" conditions. After the cesium-rich surface is obtained, typical bias conditions are restored and the main analysis can be performed with improved sensitivity. However, since any beam deceleration causes a rapid increase in its diameter, a modification of the objective lens excitation must be used to obtain a low energy caesium beam of suitable size.

This paper mainly reports on optics simulations performed with the Simion 8 package to enable the soft landing control of primary caesium ions. The practical use of this surface preparation technique is not restricted to very thin bio-samples, as it may also be useful in applications such as the improved quantification of the upper layers of the semiconductor devices prepared by shallow ion diffusion or implantation over area smaller than 5 $\mu m^2$.

## 2 Immersion objective lens: geometrical configuration

The optical simulation of the objective lens using Simion requires an accurate description of dimensions of all electrodes to be used [14,15]. Several geometries were therefore studied in succession to counterbalance any lack of accuracy in the known dimensions. Finally, the geometrical file used for Simion was extracted from a rough technical drawing of the objective lens[4].

Under the conditions that have been selected, the sample surface is placed at a distance of 0.5 mm from $E0W$, a wehnelt-like electrode with a bevelled edge on its downstream side, where "downstream" is defined according to the propagation of secondary ions. The two focussing electrodes $E0P$ and $E0S$ are followed by an electrode at ground potential including an aperture stop in the middle of its internal cavity. The electrode $E0P$ and $E0S$ openings were both set at a diameter of 6 mm and their thicknesses were set at 2 mm and 2.75 mm, respectively.

The simulation procedure was adapted to compensate for the lack of accuracy about the objective lens geometry in particular the unknown positions and size of the ion source image applied in the objective lens entrance. It is quite obvious that better geometrical parameterizations would improve the accuracy of simulations herein reported. Neither the aperture stop in the centre of the output electrode nor the unipotential lens L4 which follows the objective lens[5] have been considered.

[4] This file and the corresponding representation by Simion (see Fig. A.1) are reported in Appendix A.

[5] For the sake of conciseness, the many preliminary simulations that we performed corresponding to various complete systems will be only briefly mentioned here. In direct agreement with data from the literature [3,16,17], these initial simulations confirmed the distinct roles of electrodes $E0P$ and $E0S$ in independently focussing the primary ion probe and the secondary ions. For all studied objective lens our investigations concerned the position $x_s$ and the magnification of the image for negative ions emitted with an initial energy of 1 eV studied for a large set of emission angles (0–90°). The aperture aberrations were included as done in other simulations [14,15]. As well as for the primary ion beam, propagation was also studied in the reverse direction for positive ions leaving the sample surface with an initial energy of 16 keV, in order to evaluate the position $x_p$ and the magnification of the "antecedent", intermediate image of a punctual source at the surface centre. In practice the longitudinal position depends on the aperture angles being used. In general, the antecedent position stays at distance from objective lens larger than the secondary ion image $x_s \ll x_p$, but depending on both the geometry used and on the bias voltage, it could happen that $x_p$ is pushed as far away as the virtual antecedent $x_p < 0$.

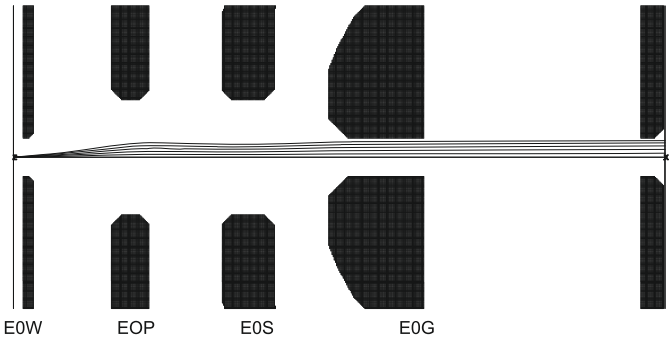


**Fig. 1.** Schematic transmission of a 16 keV ion beam leaving the substrate centre with elevation angles of 0, 1, 2, 3, 4, 5° for a lens biased using typical in conditions. Beyond emission angles of 5°, collision with the lens electrodes stops the beam transmission. For the geometry used, the beam shows a significant divergence after travelling past the objective lens. A virtual image of the "ion source" is therefore constructed at the objective entrance.

## 3 First study on the focussing of low energy probes

The approach in this first study was limited to examining meridian trajectories when employing typical bias voltages $E0W = -8000$ V, $E0P = 8500$ V and $E0S = -6950$ V. These conditions focus the 8 keV caesium beam applied in the entrance of the objective lens energy into narrow ion probes of 16 keV energy.

A first set of simulations involved propagation in the reverse direction:

In these simulations an ion beam leaves the sample centre with increasing elevation angle and with a fixed initial kinetic energy of 16 keV. Trajectories plotted within Simion show that the elevation angles of highest acceptance remain very close in value to 5° as defined relative to the sample surface (see Fig. 1).

A beam so-defined then reaches a transverse plane in the longitudinal abscissa $x_s$ (close to the usual objective

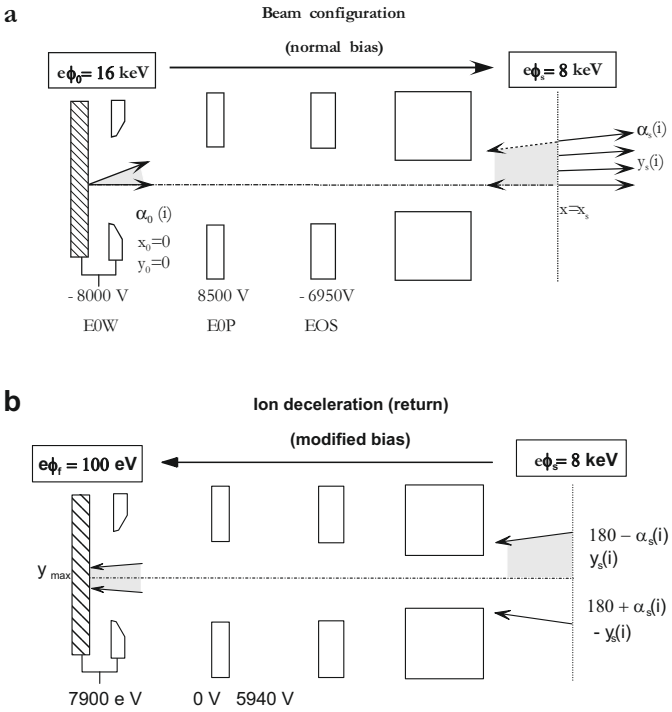


**Fig. 2.** (a) Transmission of a caesium ion beam in the reverse direction: the beam leaves the sample centre with increasing elevation angles $\alpha_0(i)$ and with an initial energy of 16 keV in order to extract the parameters $y_s(i)$ and $\alpha_s(i)$ in a fixed longitudinal position $x_s$. (b) Schematic representation of the conditions used to evalua te the focussing of a low energy ion probe. A simple modification in elevation angle is applied for a beam transmitted from right to left through the objective. During subsequent evaluation using Simion, the electrode bias voltages are modified to determine the conditions which provide the smallest beam size $y_{\max}$ reaching the sample surface with a low final energy $e\phi_f$.

lens entrance), now having new beam parameters $y_s(i)$ and $\alpha_s(i)$ and with an energy of 8 keV (see Fig. 2a). Then, a new reversal in the propagation direction was applied to a beam of 8 keV starting from $x = x_s$ and having an identical initial beam envelope $\alpha'_s(i) = 180 - \alpha_s(i)$ (see Fig. 2b). Modification of the sample voltage can be used to achieve a low final energy and new bias voltages applied to electrodes $E0P$ and $E0S$ serve to limit the size of the ion beam when arriving at the sample surface. Clearly, the independence of the two settings $E0P$ and $E0S$ opens up many possibilities and examples of the resulting variously size probes are partially summarized in Figure 3.

For a final energy of 100 eV corresponding to a given $E0S$ bias, the probe radius passes through a minimum at an $E0P$ setting of about 0 V. Obviously, as the angular limits used for the beam envelope are increased, the probe diameter is modified by the effect of the aperture aberration of the objective lens. In all cases, the 100 eV probe passes through a minimum of less than 10 $\mu$m at a bias voltage setting for the $E0P$ electrode of approximately zero volts.

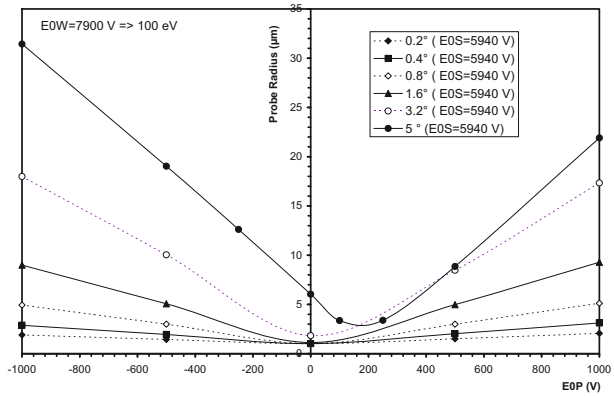


**Fig. 3.** Focussing of a caesium beam of final energy of 100 eV for a fixed $E0S$ voltage and a variable bias applied to $E0P$ electrode. The different curves correspond to various angular limits 0.2, 0.4, 0.8, 1.6, 3.2 and 5° used during beam deceleration from 8 keV to 100 eV, and for the conditions stated in Figure 2a.

## 4 Extension to a random parameterisation of ion beams

### 4.1 Calculation procedures

A similar procedure was used to study situations when the beam arrives at the entrance of the objective lens with a large number of beam particles travelling out of the meridian symmetry plane.

Under typical operating conditions for NanoSIMS, a probe of 1 $\mu$m in diameter is scanned over the sample surface[6]. Therefore, the incident beam was described by two randomly selected values of (i) initial position within a disk of radius of 0.5 $\mu$m and (ii) emission angle within a cone of half angle of 5°, 3.2°, ... (see Fig. 1, for example). This beam then arrives at the coordinates $y_s(i)$ and $z_s(i)$ on a transverse plane at a longitudinal position $x_s$ and with variable azimuth and elevation angles $az_s(i)$ and $elv_s(i)$. The simple replacement of the elevation angles by their antiparallels $(180 - elv_s(i))$ allows one to evaluate the backwards focussing of a ion probe returning to the sample with a low final energy. In practice, the "Fly2" procedure of Simion 8 was implemented to build five tables of 1000 particles, each sent through the objective as five independent set of "Ion" files[7]. This way, the implicit coherence introduced during the initial selection in elevation and position is transferred to the returned beam[8]. After these new simulations, the impact positions on the

[6] In practice the probe diameter can be set at 50 nm, but there is no direct influence on the simulations reported herein.

[7] This procedure comes from a limitation in the number of particles when building an "ion" file in Simion 8. Recently, the Simion 8.05 software was implemented to escape such limitations.

[8] A beam in the $x_s$ plane and randomly defined in position and inclination angle exhibits no coherence.

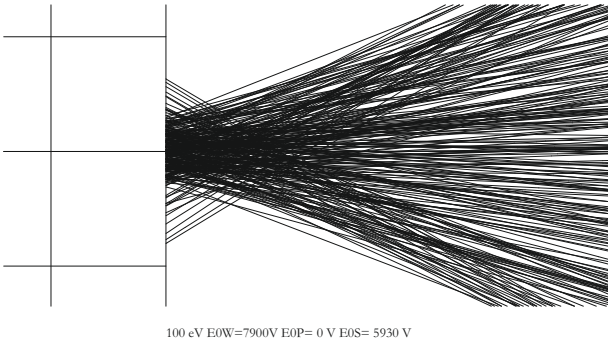


**Fig. 4.** Deceleration of a 8 keV ion beam to 100 eV ($E0W = -7900$ V, $E0P = 0$ V, $E0S = 5930$ V). This plot, produced using Simion, shows the particle paths used to adjust the objective lens focussing. The sample surface is represented on the left part as squares of $5 \times 5$ $\mu$m ($1 \times 1$ graphic unit).

sample surface are recorded as a set of $5 \times 1000$ pairs of $y(i)$ and $z(i)$.

Let us just briefly mention a preliminary control experiment, wherein the ion probe is returned to the sample surface without any modification in bias voltages. Under these conditions the beam uniformly covers an area with a diameter of 1 $\mu$m which is fairly close to the beam size used during the beam pre-configuration. However, when the sample was biased at ground potential and the usual electrode excitations were used, the returning beam covered an area as large as 110 $\mu$m in diameter and had a final energy of 8 keV.

### 4.2 Practical conditions for the adjustment of lens bias

The Simion software package offers the user the ability to directly plot particle paths. This is highly convenient when adjusting the bias voltages of the $E0S$ and $E0P$ electrodes if one applies a large magnification factor in the near vicinity of the sample surface. In practice, such direct observation is very efficient provided the number of particles stays small enough to avoid saturation effects when observed in the final display format (see Fig. 4, for example).

### 4.3 Building of an ion probe of 100 eV energy

It is now a simple task to examine the set of beam shapes obtained with the objective bias used in the procedure described previously Section 4 a ($E0W = 7900$ V, $E0P = 0$ V and $E0S = 5930$ V). As shown in the left part of Figure 5, the resulting trace diagram exhibits a small centre spot of about 3 $\mu$m surrounded by a diffused zone extending up to a diameter of 13.6 $\mu$m.

However, beam density plots may exhibit saturation in the black levels so a histogram as a function of radial distance is first build. Then, a numerical integration from the centre out to a certain radius provides the normalised density variations and the evolutions of elemental contributions as a function of radial distance. In the right part

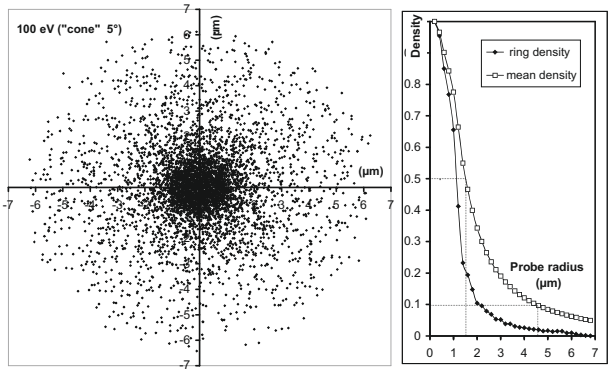


**Fig. 5.** Trace diagram reported in the left side gives positions of impacts of 5000 ions applied to the sample with a final energy of 100 eV with the bias $E0P = 0$ V, $E0S = 5930$ V. The right side plot reports the corresponding modification in density of successive rings as well as the mean density integrated from the centre up to a variable radius.

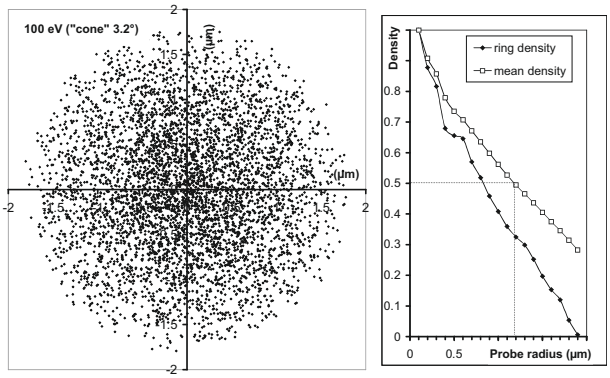


**Fig. 6.** Trace diagram reported in the left side gives positions of impacts of 5000 ions applied to the sample with a final energy of 100 eV with the bias $E0P = 0$ V, $E0S = 5930$ V (for a parameterization half angle limited to 3.2°). The right side plot reports the corresponding modification in density of successive rings as well as the mean density integrated from the centre up to a variable radius.

of Figure 5, the diagram clearly shows that about 50% and 90% of the particles remain within distances of 1.4 $\mu$m and 4.6 $\mu$m respectively.

Just as was observed when examining the aperture aberrations of the objective lens, it is straightforward to relate the particle at the edge of the arriving beam with particles emitted at the highest emission angles. Indeed, a reduction in half angle from 5° to 3.2° eliminates the diffused impacts almost completely (see Fig. 6). In addition, such conditions also reduce most variations in impact densities for the returning beam (50% and 100% of the 5000 particles are kept inside circles with radii of 1.4 and 1.9 $\mu$m respectively).

The modifications in the kinetic energies of ions when travelling along their trajectories are easily recorded using Simion for several lens bias conditions and for particles aligned along the optical axis. In Figure 7, the curve

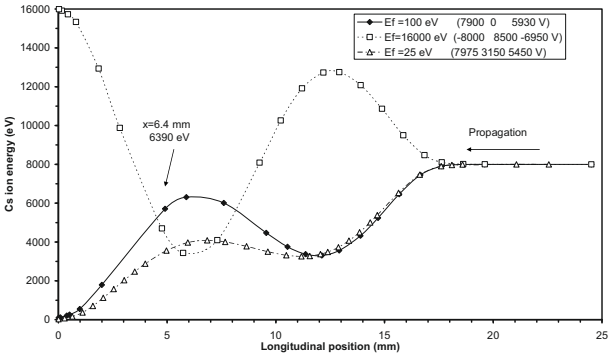


**Fig. 7.** Variation in particle energies along the objective axis. The dotted curve with open square points corresponds to typical operation conditions which provide a narrow probe of 16 keV. The continuous line with dark diamond points corresponds to conditions resulting in a 100 eV probe (see Figs. 3, 5 and 6). The line joining open triangles corresponds to a 25 eV probe.

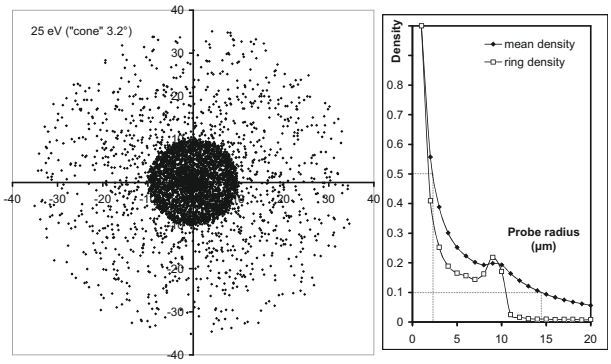


**Fig. 8.** Trace diagram build by 5000 ions of 25 eV for the objective bias voltages of $E0P = 3150$ V and $E0S = 5450$ V. The transverse extension of the centre spot depends on the lens excitation (See Tab. 2). A new limitation in the half angle less than 3.2° is assumed to significantly reduce the diffused beam.

constituted by a continuous line and dark diamond points corresponds to the conditions used in Figure 6.

Passing through the objective lens the beam first undergoes a progressive reduction in energy around the optical entrance of the objective lens ($x_s < 18$ mm). The beam then experiences a new increase in kinetic energy around $x = 12$ mm before a final deceleration occurs once it has passed $x = 5$ mm. Therefore, one might suggest that in the vicinity of electrode $E0P$ the objective lens behaves as a lens biased in acceleration mode [18]. However, as opposed to the typical deceleration bias mode, the focal points are located at relatively large distances from the optics centre, as long as the lens bias conditions provide a beam waist in close proximity to the surface. Additionally, when using typical bias mode, progressive reductions in the beam kinetic energy may lead to an increased size in the area impacted by the beam of ions. It should be added that an acceleration bias mode cannot be used to focus the primary 16 keV ion probe due to the very high voltage that would be needed to bias the $E0P$ electrode.

### 4.4 Further reduction in ion probe energies

It is very likely that a final energy as low as 100 eV may be required to caesium-enrich the sample surface prior to the main characterisation which would then use typical bias conditions. In order to further evaluate the behaviour of the immersion objective lens as a deceleration system, new reductions in ion energy were tested.

A simple simultaneous increase in the sample and the Wehnelt potential $E0W$ moves the previously obtained beam constriction far away from the surface so that the beam is partly reflected. For the previously studied lens excitations and for a final energy of 25 eV, about a third of the incident particles experience a reflection close to the sample surface. Indeed, the objective lens behaves almost as a mirror lens during the last part of particle paths. A simple modification in electrode bias voltages $E0P$ and $E0S$ restores the complete arrival of all particles and creates a small central spot surrounded by quite a large diffused area.

A decrease in the "half angle" to 3.2° is also very efficient in significantly reducing the ion impact area. The beam is entirely returned to the sample surface for a large range of bias voltages (see Tab. 1). Among all the possible bias conditions, one might consider the set of $E0P = 3150$ V and $E0S = 5450$ V which provide a centre spot surrounded by a diffused ring of about 20 $\mu$m in diameter. Therefore, the entire caesium beam is contained within an area less than 30 $\mu$m in diameter with a rather constant areal density (see Fig. 8). Such conditions are quite convenient to form a localised caesium-rich uppermost layer on a sample surface. Again, after this preparation, the sample may be easily examined using typical NanoSims conditions. Let us add that along the system axis the ions experience a variation in kinetic energy similar to that for the previously mentioned acceleration bias mode for the $E0P$ electrode (see Fig. 7). In addition, Table 2 reports other lens excitations which results in a small centre spot surrounded by a diffused impact area.

## 5 Complementary discussion

Generally speaking $Cs^+$ energies in between 25 eV and 100 eV are suitable for enriching the sample surface as the sputtering yields for these energies are well below unity [19]. As well, it is very likely that the additional limiting provided by the aperture stop in the objective lens may ease the focussing of low energy caesium beams. Keeping a low energy for the beam should reduce surface damages caused by backscattered caesium ion beams on the electrode surfaces or on the aperture stops.

To this point, the main goal of this study was to obtain a small diameter for the low energy beam corresponding to the imaged area. A diameter of about 10 $\mu$m corresponds the scanning of an ion probe of 50 nm over $200 \times 200$ pixels. Obviously if required, a small modification of electrode

**Table 1.** Influence of electrode bias on the size of returned beam (parameterisation half angle of 5°).

| Final energy(eV) | *E0W* | *E0P* | *E0S* | $R$ ($\mu$m) 50% | $R$ ($\mu$m) 90% | $R$ ($\mu$m) 100% | Transmitted fraction% |
|---|---|---|---|---|---|---|---|
| 100 | 7900 | 0 | 5930 | 1.7 | 4.6 | 6.8 | 100 |
| 50 | 7950 | 0 | 5930 | 1.7 | 4.8 | 45 | 100 |
| 25 | 7975 | 0 | 5930 | 2.7 | 6.3 | 45 | 65.7 |
| 25 | 7975 | 5450 | 5500 | 3.5 | 83 | 145 | 100 |
| 25 | 7975 | 5500 | 5600 | 5.2 | 50 | 231 | 100 |

**Table 2.** Influence of electrode bias on the size of returned beam (parameterisation half angle of 3.2°).

| Final energy(eV) | *E0W* | *E0P* | *E0S* | $R$ ($\mu$m) 50% | $R$ ($\mu$m) 90% | $R$ ($\mu$m) 100% |
|---|---|---|---|---|---|---|
| 25 | 7975 | 0 | 5930 | 2.7 | 6.3 | 45 |
| 25 | 7975 | 3200 | 5400 | 2.3 | 17 | 34 |
| 25 | 7975 | 3150 | 5450 | 2 | 15 | 36 |
| 25 | 7975 | 3050 | 5550 | 2 | 15 | 39 |
| 25 | 7975 | 3100 | 5500 | 1.6 | 10 | 37 |

biases *E0P* and *E0S* or rather a modification in potential on the usual scanning plates may be used to further enlarge the low energy caesium beam.

Clearly, during the practical experimentation many parameters will have to be evaluated:

- What is the ideal final energy and what will be the corresponding ion doses? This energy selection will obviously depend on the nature of the sample obviously. Very likely a dose about one caesium atom per surface atom will be sufficient. However, the surface concentration that will be achieved will be modified due to the implantation profile in a gradually saturated solid.
- How long will the analysis process show high sensitivity for a single preparation? Here again, the implantation profile (using 16 keV ions) of caesium-rich layers will be important. Repeated surface preparation might be necessary to maintain the best analysis conditions.
- In practice, for conductive but heterogeneous samples local variations in work function may also intervene in the very last step of the ion beam deceleration, though the chemisorption of caesium atoms may tend to reduce such effects. In any cases, variations limited to few electron-volts will barely influence the ion paths for final beam energies above 25 eV.
- Another important question concerns insulating or poorly conductive samples. Such conditions may be encountered when studying various biological materials, geological material or semiconductor surfaces including local thin oxide or silicon nitride elements.

During surface preparation the sample voltage is kept slightly higher than the *E0P* electrode bias. The local configuration of the electrostatic field creates a quasi-constant surface potential even for insulating samples provided the applied caesium beam is kept at a very low intensity. If each ion carries a single positive charge, the local emission of secondary electrons will compensate the charge imbalance, even for very low impact energies as insulating surfaces typically have large secondary electron yields.

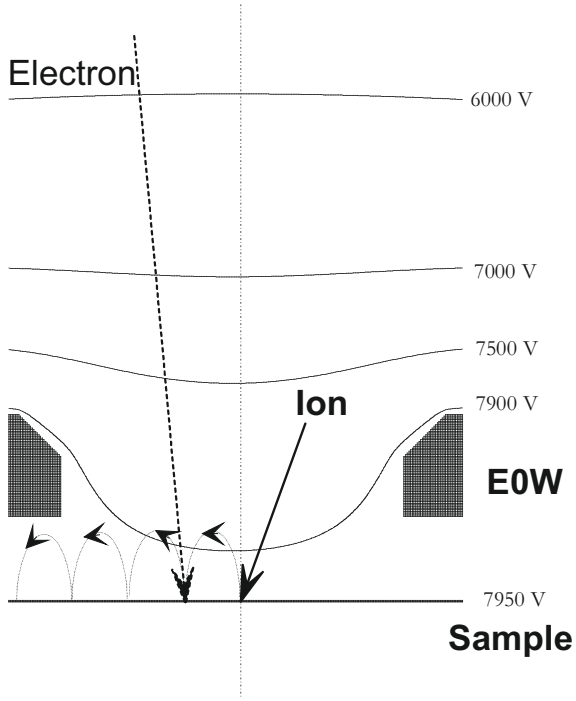


**Fig. 9.** Regulation of surface potential by secondary electrons. The equipotential surfaces shown are given by Simion for the NanoSIMS objective lens being used.

The secondary electrons ejected by the ion impact follow a parabolic path through the electrostatic field before returning to the surface to trigger new electron emissions. In this way a type of virtual electrical conductor is created close to the sample surface which keeps the sample surface potential constant really. Such surface potential control is used during SIMS analyses based on positive secondary ion emissions. These analyses, as in this study, use a high positive sample voltage applied through a coarsely spaced conducting grid evaporated on the sample surface. Such conditions provide a steady and invariant surface potential, as it is clearly shown by recording the energy distribution of positive secondary ions. In addition, the impacts of ions and neutrals on the surrounding electrodes also eject electrons which then impact the sample surface and contribute to the surface voltage regulation (see Fig. 9).

- Above all, the beam deceleration may be hindered by mechanical defects perturbing the electrostatic field in the last part of the ion paths. Indeed, one cannot exclude the possibility that the sample might be misaligned with respect to the *E0W* and *E0P* electrodes.

The machining of the $E0W$ and $E0P$ electrodes and their respective assembly could be at origin of many optical difficulties in focussing a beam of very low energy in mirror-like conditions. Nevertheless, the application of small corrections though centring plates or a small sample displacement may be necessary to align the targeted area in the centre of the secondary ion images.

– On caesium rich surfaces, a single ion impact may eject two or more secondary ions of the same species detected by the mass spectrometer as a single event by the multiplier working in pulse counting mode [9]. High ionisation yields combined with efficient ion collection and a wide energy pass band in the NanoSIMS will greatly increase the likelihood of such an event [21,22]. For dilute elements however, this simultaneous emission remains improbable and consequently no perturbation of quantification will take place. Obviously this will not be true for quantitative measurements of major elements when their electron affinities provide ionisation yields close to unity.

## Conclusion

This study has focussed on the enrichment of surfaces with caesium by directing a narrow beam of caesium ions onto the surface. The enrichment beams studied had energies as low as 100 eV, and were interrupted before the main NanoSIMS analysis was performed using caesium probe of 16 keV.

Without such preparation, the initial portion of the sample investigations is hindered by an insufficient implanted caesium content. This loss in analytical signal may be compounded by sample degradation due to atom redistributions following the bombardment with high energy $Cs^+$ ion beam.

Herein, simulations of charged particle optics performed with the Simion 8 software package have aimed to guide adjustments in the experimental setup in order to impinge a $Cs^+$ beam of very small size and with a low energy, (<100 eV) on the sample surface. Implementing such a procedure requires a simultaneous control of the sample bias voltage and of the excitation of the immersion objective lens when it is working as a projection lens for primary ions.

This study shows that a caesium probe with an energy of 100 eV may be directed into an area less than 10 $\mu$m using electrode bias voltages of 0 V and +5940 V applied to the $E0P$ and $E0S$ electrodes, respectively. The last electrode $E0P$ is shown to function in an "acceleration bias mode" which is ideal for confining the ion beam into a very small sample area. The simulations were extended to ion beams travelling out of the meridian symmetry plane: 90% of the 5000 ions impact the sample within an area 9.2 $\mu$m in diameter and with a final energy of 100 eV. Similarly for a probe of 25 eV, 90% of the beam impacts the sample within diameter below 30 $\mu$m for a small elevation angle. Here, the immersion objective lens still behaves as an acceleration lens around electrode $E0P$ bias at 3150 V whereas electrode $E0S$ is set at 5450 V.

It is clear that the accuracy of the reported simulation is limited by the used geometrical parameters. In addition, the control of an immersion objective lens under mirror-like conditions may be partly affected by small potential heterogeneities at the sample surface as well by mechanical defects affecting the mechanical assemble.

Aiming at final energies between 100 eV and 25 eV will keep the sputtering yields low enough to fix most caesium atoms very close to the sample surface. At the end of this in situ surface preparation, the main SIMS analyses may be performed with high analytical sensitivities. Obviously, new temporary disequilibria may replace the usual transitory regime build during the initial implantation of high energy caesium ions. Alternate applications of caesium ions with low energy may be used to maintain the surface concentration in caesium high enough to keep high the ion yields. Such adjustments may depend on local conditions depending on the studied material. Soon, experimental studies will complete the above simulations in charged particle optics in order to quantify the improvements in localisation and in sensitivity.

## References

1. G. Slodzian, Optik **77**, 148 (1987)
2. Ting Di Wu, thesis, Orsay, 1992; M. Bernheim, Surf. Sci. **494** 145 (2001); M. Bernheim, Surf. Sci. **566** 1221 (2004)
3. G. Slodzian, B. Daigne, F. Girard, Microsc. Microanal. Microstruct. **3**, 99 (1992)
4. M. Bernheim, J. Rebière, G. Slodzian, *SIMS II conference* (Springer Series in Chemical Physics 1979), 29
5. J. Rebière, thesis, Orsay, 1979
6. M. Bernheim, G. Slodzian, J. Microsc. Electron. **6**, 141 (1981)
7. G Slodzian, Phys. Scripta **6**, 54 (1983)
8. M. Bernheim, G. Slodzian, *SIMS VI, Proceedings* (Wiley, 1987)
9. M. Bernheim, F. Le Bourse, Nucl. Instrum. Meth. B **27** (1987)
10. M. Bernheim, G. Slodzian, *SIMS III conference* (Springer Series in Chemical Physics, 1982), 181 151
11. M. Bernheim, Rev. Phys. Appl. **24**, 94 (1989)
12. T. Wirtz, H.–N. Migeon, Surf. Sci. **561**, 200 (2004)
13. J. Brison et al., Surf. Sci. **601**, 1467 (2007)
14. M. Bernheim, Ultramicroscopy **106**, 398 (2006)
15. M. Bernheim, Eur. Phys. J. Appl. Phys. **36**, 193 (2006)
16. G. Slodzian, B. Daigne, F. Girard, F. Boust, F. Hillion, Bio Cell **74**, 43 (1992)
17. C. Lechene et al., J. Biol. **5**, 20 (2006)
18. G. Slodzian, A. Figueras J. Phys. Lett. **39**, L90 (1978)
19. H.H. Andersen, H.L. Bay, *Topic in Applied Physics47: Sputtering by particle bombardments*, edited by R. Beyrich, I 164 (1981)
20. G. Slodzian et al., Eur. Phys. J. Appl. Phys. **14**, 199 (2001)
21. G. Slodzian, Surf. Sci. **231**, 3 (2004)

## Appendix A: Example of geometrical file used with Simion

```
; NanoSIMS (0.5 3+3); scale 204 Gu =1mm

Pa_Define(6910,4500,1,C,Y)

Locate(0,0)
{E(1))      ; Substrate surface + E0W (guard electrode and bevelled edge
      {Fill {     Within      {Box(0,0,2,4500)}
                  Within      {Polyline
(102,4500,102,204,173,204,224,255,224,3600,320,4140,620,4500)}}}}

Locate(1040,0)          ; E0P  Ion probe focussing r= 3 mm
{E(2)
      {Fill {     Within      {Polyline
(0, 714, 102, 612, 310, 612, 408, 714, 408, 2350, 433, 2600, 560, 2856,
840, 3136, 1632, 4030, 1734, 4386, 1734, 4500, 1122, 4500, 918, 4500, 918,
3930, 870, 3826, 204, 3160, 50, 2856, 0, 2601)}}}}

Locate(2210,0)          ; E0S Focussing of secondary ions r= 3 mm

{E(3)
      {Fill{      Within      {Polyline
(0, 714, 102, 612, 458, 612, 560, 714, 560, 1530, 612, 1785, 714, 1938,
1683, 2907, 2193, 3570, 2346, 3876, 2346, 4500, 1580, 4500, 1580, 3876,
1480, 3468, 1326, 3213, 255, 2142, 153, 1938, 0, 1530)}}}}

Locate(3335,0)          ; Ground potential electrode
{E(0)
      {Fill{      Within      {Polyline
(0,408,204,204,1020,204,1020,1682,1938,2600,3315,2600,3315,204,3468,204,357
0,306,3570,3009,3570,4500,1938,4500,1938,3620,1836,3162,1683,2907,280,1504,
102,1173,0,918)}}}}
```

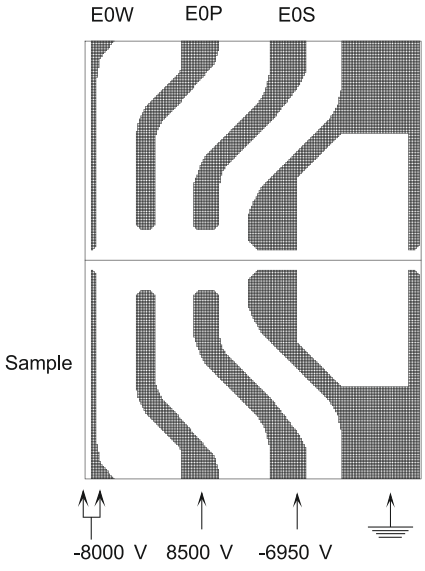


**Fig. A.1.**